Thermochimica Acta 518 (2011) 111–118

Contents lists available at ScienceDirect

Thermochimica Acta

journal homepage: www.elsevier.com/locate/tca

Thermodynamics of U(VI) and Eu(III) complexation by unsaturated carboxylates

Neetika Rawat[a], A. Bhattacharyya[a], B.S. Tomar[a,*], T.K. Ghanty[b], V.K. Manchanda[a]

[a] *Radiochemistry Division, Bhabha Atomic Research Centre, Mumbai 400085, India*
[b] *Theoretical Chemistry Section, Bhabha Atomic Research Centre, Mumbai 400085, India*

ARTICLE INFO

Article history:
Received 11 December 2010
Received in revised form 25 January 2011
Accepted 11 February 2011
Available online 19 February 2011

Keywords:
U(VI)
Eu(III)
Unsaturated carboxylates
Calorimetry
Thermodynamics
Complexation

ABSTRACT

The thermodynamic parameters (ΔG, ΔH and ΔS) of complexation of U(VI) and Eu(III) by unsaturated dicarboxylic acids, namely, maleic and fumaric acid, has been determined by potentiometric and microcalorimetric titrations at fixed ionic strength ($I = 1.0$ M) and temperature (298 K). The results show formation of 1:1 complexes by both the ligands with Eu(III). In the case of U(VI), maleate forms both 1:1 and 1:2 complexes, while only 1:1 complex was formed with fumarate. The fluorescence emission spectra of Eu(III)–dicarboxylate solutions at varying ligand to metal ratio were also used to obtain their stability constants. In addition, the fluorescence lifetimes reveal higher dehydration of Eu(III)–maleate compared to Eu(III)–fumarate which corroborates the ΔS values. The thermodynamic quantities suggest charge polarization effects in the case of U(VI) and Eu(III) complexes of fumarate, which is further corroborated by theoretical calculations. For the same ligand, U(VI) complexes were found to be more stable which was mainly due to higher entropy term.

1. Introduction

Studies on the complexation of actinides by carboxylic acids (mono, di, hydroxy) have attracted considerable interest during the recent past mainly due to two reasons. (i) Carboxylic acids present in the natural waters may play important role in influencing the migration of actinides in the aquatic environment around the deep geological repository [1–3]. They are also used as model compounds to investigate the mechanism of binding of actinides by humic substances in the natural waters [4–6]. (ii) Hybrids containing rare earths and organic moieties have been found to enhance the optical properties of rare earth elements. For instance, luminescence of Eu(III) was found to be sensitized by complexation with carboxylic acids [7–9].

Actinides present in the nuclear waste are considered most important from waste management point of view due to their long half life and alpha emitting properties. The fate of actinides in environment depends on their interaction with various organic and inorganic ligands present in the aquatic environment. Among the organic ligands, humic acid, fulvic acid and some of the simple carboxylates are most predominant. Though a lot of data on stability constant is available, the complete thermodynamic parameters are scarcely available. These parameters not only help in understanding the coordination of actinides in complexed form but are also required to determine log K at higher temperatures.

Kirishima et al. recently studied the complexation of Eu(III) and U(VI) with various mono-carboxylates, di-carboxylates and hydroxy carboxylates using potentiometry and calorimetry [10]. Complexation of U(VI) by oxalate and gluconate have been studied recently by the Berkeley group led by Rao [1,2]. Kitano et al. determined the thermodynamic parameters of the complexation of Eu(III) by di-carboxylates and hydroxyl-carboxylates and obtained linear correlation between the entropy of complexation and the number of coordinated water molecules around the central metal ion [11]. We have recently studied the thermodynamics of complexation of Eu(III) by carboxylates using isothermal titration calorimetry [12]. Time resolved fluorescence spectroscopy was also used to obtain the stoichiometry of the Eu(III) complexes along with the stability constants [6]. With the availability of intense light sources in the form of synchrotrons, there has been resurgence in the determination of molecular structure of actinide complexes. X-ray absorption fine structure spectroscopy (XAFS), time resolved fluorescence spectroscopy (TRFS) and NMR spectroscopy are being widely used to understand the mechanism of coordination of the metal ion by the ligands [13–15]. The complexation of actinides by unsaturated carboxylates is relatively less understood. The rigidity in unsaturated ligand and ease of charge polarization makes their chemistry interesting and different from saturated carboxylates. Choppin et al. have determined thermodynamic parameters (ΔG, ΔH and ΔS) of Eu(III) complexation with maleate and fumarate and attributed the higher stability of some of the carboxylates to charge polarization [16]. Ramamoorthy and Santappa determined the stability constants of U(VI) complexes with maleate and fumarate [17]. The data on enthalpy and entropy of U(VI)

---

* Corresponding author. Tel.: +91 22 25595006; fax: +91 22 25505151.
E-mail address: bstomar@barc.gov.in (B.S. Tomar).

0040-6031/$ – see front matter © 2011 Elsevier B.V. All rights reserved.
doi:10.1016/j.tca.2011.02.018

complexes with these carboxylates are not available in the literature. The coordination of UO_2^{2+} by the carboxylate anion occurs in the equatorial plane unlike in the case of Eu(III) where coordination occur through spherical coordination space. With this in view thermodynamic parameter of complexation of U(VI) by maleate and fumarate were determined by potentiometry and calorimetry. Though the thermodynamic data for Eu(III) complexation with maleate and fumarate are known. They were determined under same experimental condition as for U(VI) for comparison purpose. The time resolved fluorescence studies on Eu(III) complexes were also carried out to determine their stability constants. In addition the fluorescence lifetime data have been used to obtain information about inner sphere coordination of Eu(III) in complexes. Eu(III) is commonly used as a chemical analogue of trivalent actinides, with regard to their environmental chemistry. In order to understand charge distribution on ligands and complexes, ab initio calculation for charge distribution on all the atoms of ligand as well as complex has been carried out by natural population analysis in TURBOMOLE. The stability constants have been compared with that for other carboxylates to investigate the mechanism of the complex formation. The enthalpy and entropy of complexation have been explained in terms of the hard acid–hard base theory of actinide carboxylate complexation.

Table 1
Titration conditions for Eu(III) and U(VI) complexation with fumarate and maleate at $I = 1.0$ M and 25 °C.

S. No.	Cup solution		Titrant	
	C_M (mM)	C_H (M)	C_L (M)	C_H (M)
(a) Potentiometric titration (cup volume = 20.0 ml)				
Eu(III)–fumarate	1.00	0.007	0.500	0.186
	3.00	0.012	0.500	0.186
	4.95	0.016	0.500	0.186
Eu(III)–maleate	3.00	0.011	0.500	−0.009
	5.00	0.016	0.500	−0.009
U(VI)–fumarate	3.00	0.022	0.499	0.150
	5.00	0.023	0.499	0.150
U(VI)–maleate	0.99	0.022	0.500	0.077
	3.04	0.022	0.500	0.077
	4.99	0.022	0.500	0.070
(b) Calorimetric titration (cup volume = 2.7 ml)				
Eu(III)–fumarate	3.00	0.012	0.500	0.186
	4.95	0.016	0.500	0.186
Eu(III)–maleate	3.00	0.011	0.500	−0.009
	5.00	0.016	0.500	−0.009
U(VI)–fumarate	3.00	0.022	0.499	0.150
U(VI)–maleate	0.99	0.022	0.500	0.077
	3.04	0.022	0.500	0.077

2. Experimental

2.1. Reagents

Analytical reagent grade Eu_2O_3 (Merck) was used to prepare the stock solution of Eu(III) (~0.1 M) in dilute perchloric acid. Uranium stock solution (~0.1 M) was prepared from the spectroscopically pure U_3O_8. Analytical reagent grade (Merck) maleic acid and fumaric acid were used for preparation of the ligand solutions. MilliQ water having resistivity of 18 MΩ cm was used to prepare all solutions. Ionic strength of the solutions was maintained using analytical reagent grade $NaClO_4$ as a supporting electrolyte. The pH of the solutions was adjusted by addition of 0.1 M $HClO_4$ or 0.1 M NaOH. The concentration of the Eu(III) stock solution was determined accurately by complexometric titration of the metal ion solution with EDTA solution of known concentration and using Xylenol orange as an indicator. U(VI) stock solution was standardized by spectrophotometry using bromo-PADAP as a chromogenic reagent.

2.2. Potentiometric titrations

All the potentiometric titrations were carried out at 298 K using the Metrohm autotitrator (Model no.716 DMS Titrino). The electrolyte solution of the glass electrode (KCl) was replaced by 1 M NaCl solution to prevent precipitation of $KClO_4$ and hence clogging of the frit. Prior to each potentiometric titration the glass electrode was calibrated using titration of standard $HClO_4$ (~0.01 M) and standard NaOH (~0.1 M). The emf of the electrode was recorded as a function of the volume of the base and the emf (*e.m.f*) vs. pH showed a linear plot representing Eqs. (1) and (2) for acidic and basic regions respectively.

$$e.m.f = e.m.f.^0 + \frac{RT}{F}\ln[\mathrm{H}^+] + \gamma_\mathrm{H}[\mathrm{H}^+] \qquad (1)$$

$$e.m.f = e.m.f.^0 + \frac{RT}{F}\ln K_w - \frac{RT}{F}\ln[\mathrm{OH}^-] + \gamma_\mathrm{OH}[\mathrm{OH}^-] \qquad (2)$$

where $\gamma_H[H^+]$ and $\gamma_{OH}[OH^-]$ are electrode junction potential for hydrogen ion and hydroxide ion. *R* is the gas constant, *F* is the Faraday constant and *T* is the temperature in Kelvin.

The acid concentration of the Eu(III) stock solution was determined by titration of the solution with standard NaOH (~0.1 M) solution and following Gran's method [18]. The protonation constant of the di-carboxylic acids was determined by the potentiometric titration of the acid solution (~0.005 M) by NaOH (~0.1 M) or potentiometric titration of sodium dicarboxylate (~0.005 M) with standard $HClO_4$ (~0.1 M). For complexation constants the metal ion solution in pH range 1–2 were titrated with ligand solution. The conditions of potentiometric titrations for complexation are given in Table 1a. The potentiometric titration data were analysed using the software HYPERQUAD 8.0 [19] to obtain the stepwise stability constants ($\log K_j$) of the complexes.

2.3. Calorimetric titrations

The calorimetric experiments were conducted with an isothermal titration calorimeter system (Nanocalorimeter TAM-III, Thermometric AB, Sweden). It is a twin thermopile heat conduction type calorimeter and differential power signal measured is dynamically corrected for the thermal inertia of the system. The titration assembly consists of 4 ml reaction vessel and a reference vessel. The heat capacity of reaction vessel and reference vessel is balanced by keeping the same volume of solutions in both sides in order to minimize the short-term noise. The titrant is delivered in the reaction vessel through a stainless steel injection needle (length 1 m and internal diameter 1.5×10^{-4} m) connected to the Hamilton syringe containing the titrant. The syringe was driven by Lund Syringe pump. The temperature of the bath was maintained at 25.0000 (±0.0001) °C. The instrument was calibrated electrically and the performance of the instrument was tested by measuring $\log K$ and ΔH for the reaction between $BaCl_2$ and 18C6 in water. The details of the calorimeter are given in [20].

Calorimetric titration of sodium maleate and sodium fumarate solutions (0.01 M) with standard $HClO_4$ was carried out to determine the enthalpy of protonation of the acids. For the calorimetric titration of Eu(III) or U(VI) solution with the di-carboxylate, the metal ion solution (0.001–0.005 M) at the desired pH and ionic strength was taken in the reaction vessel and was titrated with the ligand solution (Table 1b). The heat of dilution of titrant was determined by in a separate calorimetric titration of the blank electrolyte solution ($I = 1.0$ M $NaClO_4$) with the titrant solution. At each step of titration, the net reaction heat Q_i^r, was calculated using the equation:

$$Q_i^r = Q_i^{\exp} - Q_i^{\mathrm{dil}} \tag{3}$$

The dilution corrected calorimetric titration data were analysed to obtain the enthalpy changes in the reaction. The $\log K_j$ values for the step wise complexation reactions were obtained from the potentiometric titration experiments.

2.4. Time resolved fluorescence spectroscopy (TRFS) measurements

The main aim of the TRFS measurements was to obtain stability constant from emission spectra and to determine the number of water molecules in the primary coordination sphere of the Eu(III) carboxylate complex which, in turn, provides information about the number of ligand anions complexed to the central metal ion. For this purpose, a TRFS instrument from Jovin Yuon (Sweden) was used. The excitation source is a xenon flash lamp having a frequency of 10 Hz. The excitation wavelength was selected at 396 nm, while the emission spectra were recorded in the wavelength range of 560–640 nm. The monochromatic light from the source falls on the 1 cm thick quartz cell and the fluorescence light emitted at 90° is monitored by an array of diode detectors cooled to −26 °C by Peltier cooling method. The fluorescence decay spectra were collected in a 2048 channel analyser with a time calibration of 1 μs per channel. The fluorescence decay spectra were fitted into multi-exponential function to obtain the lifetime of the excited state $^5D_0$ of Eu(III). In the case of U(VI) the fluorescence spectroscopic measurements could not be carried out owing to the quenching of fluorescence by carboxylates.

2.5. Theoretical calculations

All the calculations were carried out using TURBOMOLE program package [21] where for the heavy atoms 28- and 60-electron core pseudo potentials (ECP) along with corresponding (14s13p10d8f1g)/[10s9p5d4f1g] basis set were selected for Eu and U respectively [22–26]. All other lighter atoms were treated at the all electron (AE) level and the standard def-SV(P) basis sets as implemented in the TURBOMOLE program was used. Geometries of the free fumarate and maleate ligands and their complexes with Eu^{3+} and $UO_2{}^{2+}$ ions were fully optimized without any symmetry constraint at the density functional level of theory using Becke's exchange functional [27] in conjunction with Perdew's correlation functional [28] (BP86) with generalized gradient approximation (GGA). The charge distribution was calculated by natural population analysis in TURBOMOLE.

3. Results and discussion

3.1. Protonation of ligands

The protonation constants of maleate and fumarate anions were determined by fitting of the potentiometric titrations using the HYPERQUAD 8.0. The data are reported in Table 2 and are in good agreement with the literature data [17]. The calorimetric titration data for fumarate is shown in Fig. 1. The Q_i^r for protonation of fumarate were positive initially and later became negative indicating stepwise enthalpies, ΔH_{P1} and ΔH_{P2}, to be endothermic and exothermic respectively. The Q_i^r can be related to ΔH_{P1} and ΔH_{P2} by following relation:

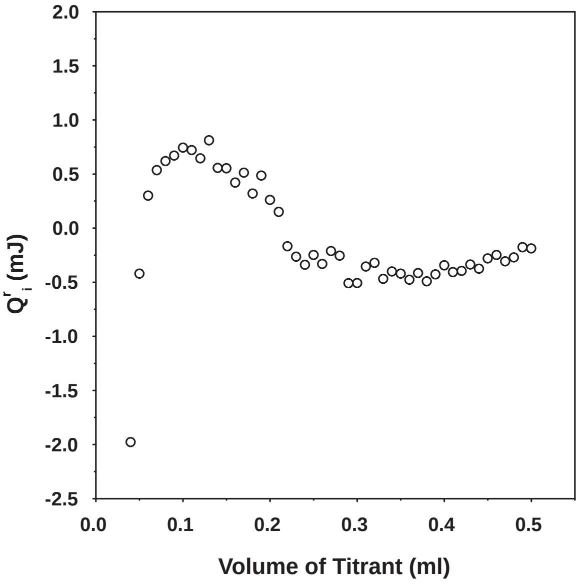

Fig. 1. Calorimetric titration of fumarate solution ($C_L = 6.6 \times 10^{-3}$ M, $[OH^-] = 1 \times 10^{-4}$ M) with 0.098 M $HClO_4$.

$$Q_i^r(\mathrm{Cal}) = \Delta \mathrm{H}_{P1}(\nu_i^{HL} - \nu_{i-1}^{HL}) + (\Delta \mathrm{H}_{P1} + \Delta \mathrm{H}_{P2})(\nu_i^{H_2L} - \nu_{i-1}^{H_2L}) + (\Delta \mathrm{H}_n \cdot \Delta \nu_{\mathrm{H_2O}}) \tag{4}$$

where ν_i^X is the number of moles of species '*X*' in the cup after *i*th injection and ΔH_n is the enthalpy of neutralization.

The $\log K_{P1}$ of maleate was found to be higher than that of fumarate, while in the case of $\log K_{P2}$ the order was reversed. The increased electron density of the maleate molecule due to cis configuration of carboxylate group's makes protonation favourable compared to fumarate. However, after first protonation the intramolecular hydrogen bonding in maleate makes second protonation less favourable.

The free energies of dicarboxylates and its mono and di protonated forms, $E(L^{2-})$, $E(LH^-)$ and $E(LH_2)$, respectively, calculated by ab initio molecular orbital theory are given in Table 3. The free energy of first protonation ΔE_1 $(E(HL) - E(L^{2-}))$ is more negative for maleate than that for fumarate while in the case of second protonation ΔE_2 $(E(LH_2) - E(LH^-))$, the trend is reversed. The higher charge density of maleate molecule results in higher $E(L^{2-})$ for maleate compared to that for fumarate. However, stabilization of mono-protonated maleate by intramolecular hydrogen bonding leads to lower $E(LH^-)$ in maleate compared to that in fumarate. Thus, the more negative

Table 2
Thermodynamic data for protonation of maleate and fumarate at *I* = 1.0 M and 25 °C.

Reaction	Log K_P	ΔH_P (kJ/mol)	ΔG_P (kJ/mol)	$T\Delta S_P$ (kJ/mol)
Fumarate				
$L^{2-} + H^+ = LH^-$	3.98 ± 0.01 (4.11)[a]	1.04 ± 0.103	−22.71	23.75
$LH^- + H^+ = LH_2$	2.91 ± 0.01 (2.89)[a]	−1.10 ± 0.116	−16.60	15.50
Maleate				
$L^{2-} + H^+ = LH^-$	5.66 ± 0.01 (6.16)[a]	0.28 ± 0.057	−32.30	32.58
$LH^- + H^+ = LH_2$	1.7 ± 0.01 (1.95)[a]	1.4 ± 0.2	−9.70	11.10

[a] Ref. [17].

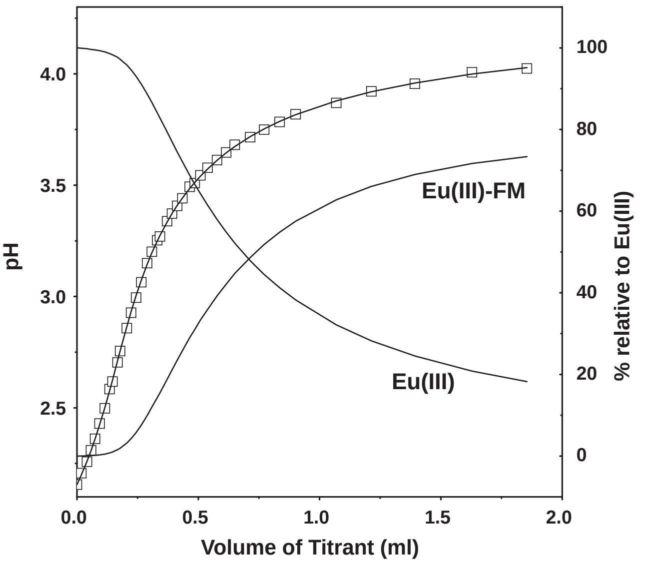

Fig. 2. Potentiometric titration of Eu(III) solution (C_M = 4.95 mM in 0.007 M $HClO_4$) with fumarate solution (C_L = 0.5 M and C_H = 0.186 M).

$\Delta E_1 - \Delta E_2$ for maleate is a result of intramolecular hydrogen bonding.

The ΔH_{P1} and ΔH_{P2} for both the dicarboxylates are found to be close to zero indicating that protonation is driven mainly by entropy. The ΔH_{P1} is more endothermic than ΔH_{P2} for most of the di-carboxylates studied by Kirishima et al. [10]. The higher dehydration energy associated with the first protonation makes it more endothermic. Similar trend is observed for fumarate. However reverse trend was obtained for maleate and phthalate, which could be due to intramolecular hydrogen bonding in mono protonated maleate and phthalate.

3.2. Complexation studies

The potentiometric titration data for Eu(III) and U(VI) carboxylates were analysed by HYPERQUAD 2008 and the two representative set of potentiometric data along with the speciation diagram are given in Figs. 2 and 3 respectively.

The calorimetric titration data for complexation, Q_i^r, in conjunction with speciation obtained using stability constant ($\log K_j$) were used to obtain enthalpy of complexation (ΔH_j). For instance, in the case of complexation reaction involving ML and ML_2 species, the Q_i^r is related to the stepwise enthalpy of complexation, ΔH_j (j = 1, 2), by Eq. (5).

$$\begin{aligned} Q_i^r &= \Delta H_1(\nu_i^{ML} - \nu_{i-1}^{ML}) + (\Delta H_1 + \Delta H_2)(\nu_i^{ML_2} - \nu_{i-1}^{ML_2}) \\ &\quad + \Delta H_{P1}(\nu_i^{HL} - \nu_{i-1}^{HL} - C_{HL}V_i) \\ &\quad + (\Delta H_{P1} + \Delta H_{P2})(\nu_i^{H_2L} - \nu_{i-1}^{H_2L} - C_{H_2L}V_i) \end{aligned} \quad (5)$$

Table 3
Theoretically calculated free energies of protonation of ligands.

Ligand	ΔE_1 ($E(LH^-) - E(L^{2-})$) (kJ/mol)	ΔE_2 ($E(LH_2) - E(LH^-)$) (kJ/mol)	$\Delta E_1 - \Delta E_2$ (kJ/mol)
Maleate	−1857.21	−1336.53	−520.682
Fumarate	−1736.97	−1404.89	−332.072

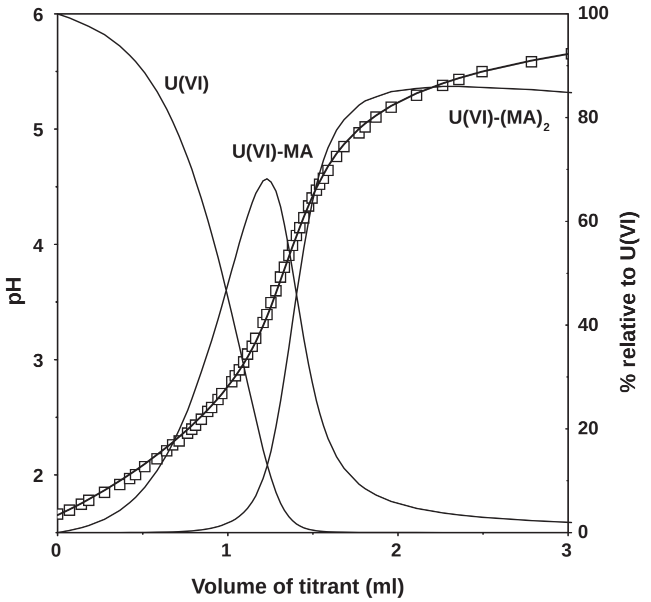

Fig. 3. Potentiometric titration of U(VI) solution (C_M = 5 mM in 0.022 M $HClO_4$) with maleate solution (C_L = 0.5 M and C_H = 0.071 M).

C_{HL} and C_{H_2L} are the concentrations of mono-protonated and di-protonated ligand in the titrant respectively. The stability constant (K_i) and protonation constant (K_P) obtained from potentiometric titrations were used to calculate ν_i for all species. ΔH_j for Eu(III) and U(VI) carboxylates were obtained by non linear square fitting of the Q_i^r data (Eq. (5)).

3.2.1. Eu(III) carboxylates

The potentiometric titration data reveal the formation of only 1:1 complex in the case of Eu(III)–maleate and Eu(III)–fumarate. The stability constants obtained for Eu(III) are given in Table 4 along with the literature data wherever available. The $\log K$ and ΔH values for Eu(III)–maleate and Eu(III)–fumarate complexes are lower than that reported by Choppin et al. [16]. The difference between the thermodynamic data can be explained on the basis of the different ionic strengths used in the two studies. The plots of $\log K_P$ vs. $\log K_1$ for some mono-carboxylates along with fumarate and maleate complexes are given in Fig. 4a. The data for other carboxylates are taken from the literature [29]. As the metal–ligand interactions are mainly electrostatic in nature, the $\log K_1$ for mono-carboxylates vary linearly with $\log K_P$. The $\log K$ for both Eu(III)–maleate and Eu(III)–fumarate complexes are above the line. The higher stability constant of Eu(III)–maleate can be clearly attributed to chelate formation. However, in case of Eu(III)–fumarate, the chelation is not possible because of trans configuration. The $\log K_1$ of Eu(III)–fumarate falls in line when plotted against $\log K_{P1} + \log K_{P2}$. This indicates the participation of charge density from both the carboxylate groups of fumarate, which could be due to polarization of electronic charge through conjugated π system [16].

To validate the above hypothesis, the structures of fumarate, maleate and their 1:1 complexes with Eu^{3+} and UO_2^{2+} were optimized. The calculated charge distribution on different atoms in the complex is given in Fig. 5. In case of fumarate, the negative charge on non bonding carboxylate oxygen atoms (O_3/O_4) was found to reduce from (−0.781/−0.784) to (−0.434/−0.360) and (−0.544/−0.499) on complexation with Eu^{3+} and UO_2^{2+} respectively. The decrease in charge from +3 to +1.759 on Eu^{3+} and from 2.0+ to +0.845 (+1.99 on U and −0.57 on each of the axial 'O' atoms) on UO_2^{2+} on complexation with fumarate, also points towards polarization of electron charge density from non bonding carboxylate to bonding carboxylate. The charge distribution of fumarate complex suggests that the complexation of metal ion proceeds

Table 4
Thermodynamic data for complexation of Eu(III) and UO_2^{2+} with maleate and fumarate at $I = 1.0$ M and 25 °C.

Reaction	Log K	ΔH (kJ/mol)	ΔG (kJ/mol)	$T\Delta S$ (kJ/mol)	τ (μs)	Δn
Maleate						
$Eu^{3+} + L^{2-} = EuL^{+}$	3.15 ± 0.04 (3.14 ± 0.06)[a] (3.83)[b]	10.9 ± 0.3 (14.21)[b]	−17.97	28.8	158 ± 2	2.9
Fumarate						
$Eu^{3+} + L^{2-} = EuL^{+}$	2.35 ± 0.03 (2.15 ± 0.03)[a] (2.86)[b]	10.1 ± 0.5 (14.37)[b]	−13.41	23.5	128 ± 3	1.3
Maleate						
$UO_2^{2+} + L^{2-} = UO_2L$	4.63 ± 0.04 (4.46)[c], (5.15)[d]	20.4 ± 0.4	−26.43	46.8	–	–
$UO_2L + L^{2-} = UO_2L_2^{2-}$	2.99 ± 0.024	7.3 ± 0.3	−17.07	24.4	–	–
Fumarate						
$UO_2^{2+} + L^{2-} = UO_2L$	2.92 ± 0.03 (3.05)[d]	10.9 ± 0.44	−16.67	27.6	–	–

[a] Obtained by fluorescence spectroscopy.
[b] Ref. [16].
[c] Ref. [31].
[d] Ref. [17].

through participation of electron charge density from both the carboxylate group thus supporting the experimental observation. In case of Eu(III)–maleate, the charge on Eu^{3+} was reduced from +3 to +1.906 on complexation and in the UO_2–maleate complex, the charge on UO_2^{2+} reduced from 2+ to +0.874 on complexation. In spite of lower transfer of charge from the ligand to the metal ion, maleate shows higher stability constant as compared to fumarate and it can be attributed to the formation of stronger 7-membered chelate ring in case of maleate complexes.

The ΔH value is similar for Eu(III)–fumarate and Eu(III)–maleate and the higher stability of latter is due to higher ΔS. The higher dehydration of metal ion and higher metal ion–ligand interaction in Eu(III)–maleate compared to Eu(III)–fumarate has opposing effect on ΔH. However higher dehydration of the metal ion and ligand anion increases the ΔS for Eu(III)–maleate complexation.

The fluorescence spectra and lifetime in the case of Eu(III) complexes were measured as a function of the volume of titrant. The spectra have been normalized to the intensity of 592 nm peak. Fig. 6a shows some of the normalized fluorescence emission spectra of Eu(III)–maleate system recorded during the fluorescence spectrometric titration of Eu(III) with maleate. The fluorescence decay profiles at two ligand concentrations are shown in Fig. 6b. The 616 nm peak corresponds to hypersensitive transition ($^5D_0 \rightarrow {}^7F_2$) and its intensity with respect to 592 nm peak ($^5D_0 \rightarrow {}^7F_1$) increases with complexation owing to its electric dipole nature. The ratio of intensities of 616 to 592 nm peaks, known as the asymmetric ratio (AR) is a measure of the asymmetry of the complex. The AR was found to increase with the volume of the titrant (Fig. 7a), indicating the formation of Eu(III)–maleate complex. Similar data were obtained in the case of Eu(III)–fumarate also (Fig. 7b). The stability constant of Eu(III) complexes with maleate and fumarate were obtained by analysing these spectra using the HYPERQUAD 2006. The log K values are given in parenthesis in Table 4 and are in good agreement with those obtained by potentiometry, except that the errors are higher, which is attributed to the scatter in the intensity ratios.

Fig. 7a and b also shows the variation of fluorescence decay lifetime with the volume of titrant for Eu(III)–maleate and fumarate systems respectively. The single lifetime obtained during the titration indicates the fast exchange of ligand between free and complexed metal ion. The lifetime increases with volume of titrant as more and more complex is formed and finally saturates at 158 and 128 μs for Eu(III)–maleate and Eu(III)–fumarate respectively. The lifetime data can be related to number of water molecules present in inner coordination sphere of Eu(III) by the following empirical formula [30],

$$N_{H_2O} = \left(\frac{1.07}{\tau}\right) - 0.62 \qquad (6)$$

The number of water molecules coordinated to Eu(III)–maleate and Eu(III)–fumarate are 6.1 and 7.7 respectively. The higher lifetime of Eu(III)–maleate compared to Eu(III)–fumarate supports the higher dehydration of Eu(III) in Eu(III)–maleate than in Eu(III)–fumarate. The number of water molecules removed (Δn)

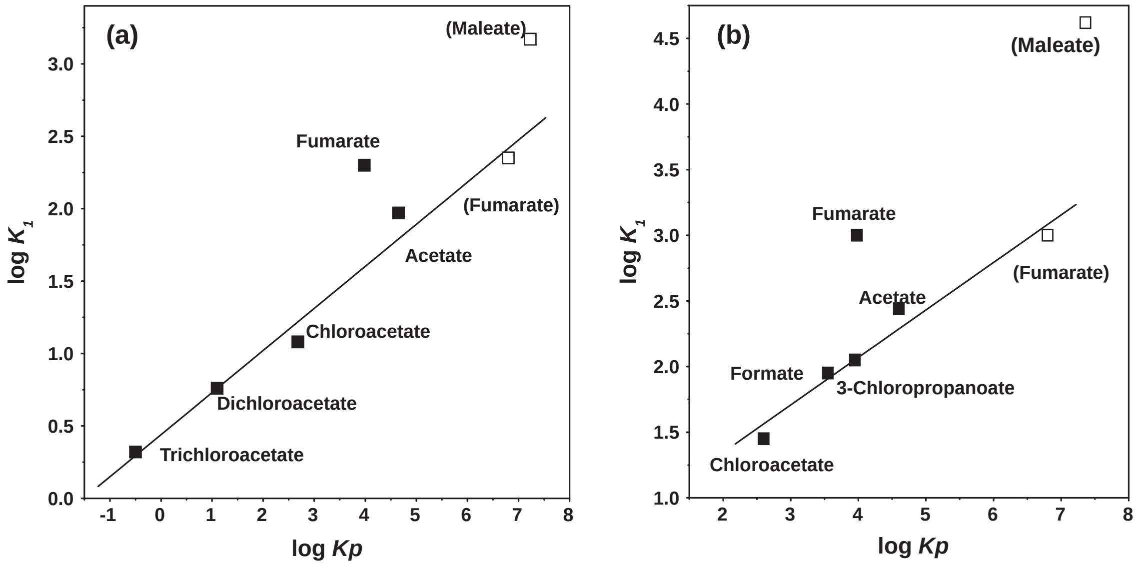

Fig. 4. Plot of log K_1 vs. log K_P for (a) Eu(III) carboxylates and (b) U(VI)–carboxylate. Data in parenthesis: plotted vs. (log K_{P1} + log K_{P2}).

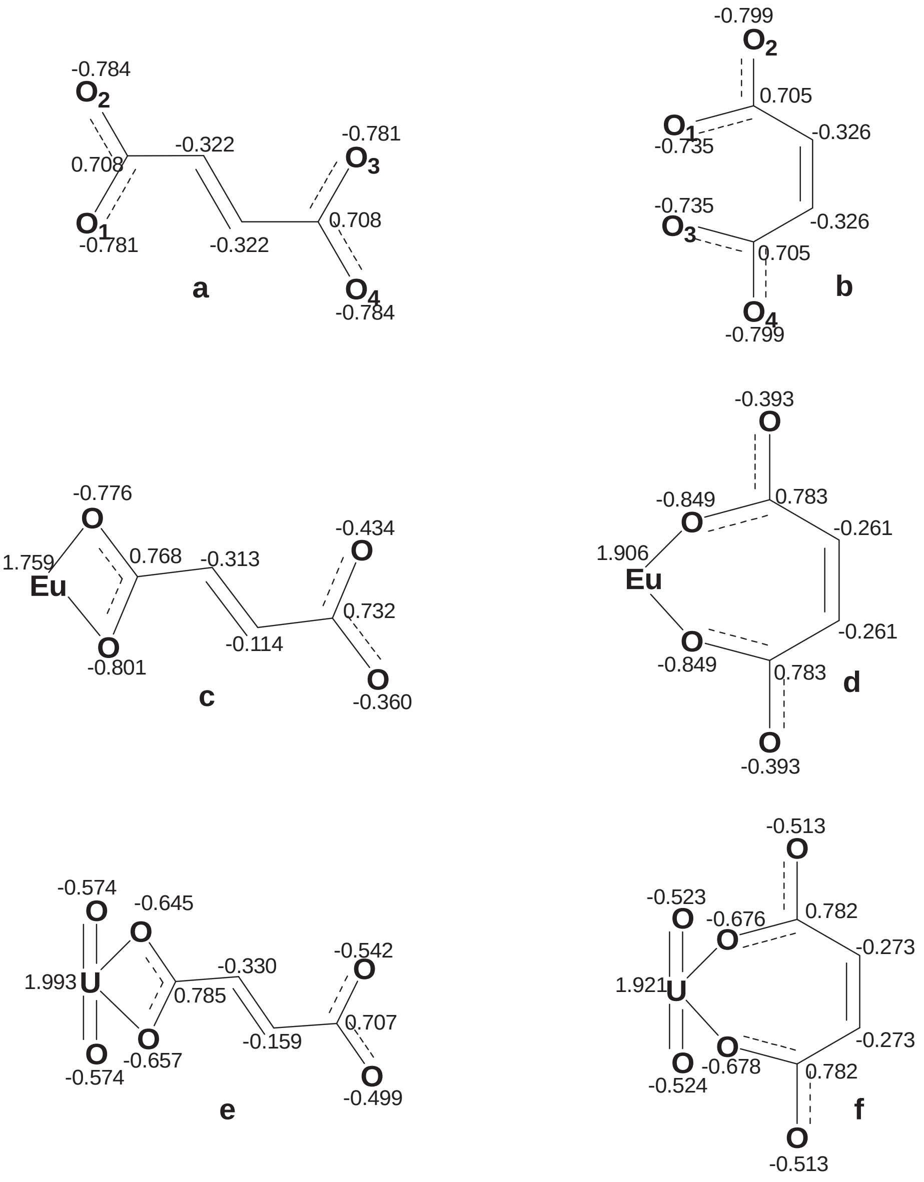

Fig. 5. NPA atomic charges of free fumarate (a) and maleate (b) and their 1:1 complex with Eu^{3+} (c and d) and UO_2^{2+} (e and f).

during complexation of Eu(III) by fumarate indicates binding similar to acetate for which fluorescence lifetime has been reported to be 133 μs [11].

The basicity of ligand and ring size of the chelate are the two main factors which determine the thermodynamic parameters. Eu(III)–succinate and Eu(III)–maleate have similar ΔH values as well as ring size with the former having higher basicity [10,12]. The higher basicity of succinate in Eu(III)–succinate is compensated by rigid structure of maleate in Eu(III)–maleate, thus resulting in similar thermodynamic parameters.

3.2.2. U(VI)–carboxylates

The analysis of potentiometric data revealed formation of 1:1 complex in U(VI)–fumarate while in the case of U(VI)–maleate the formation of 1:1 and 1:2 complexes was observed. The measured $\log K$ values are given in Table 4 along with the literature data [17,31]. In general, there is good agreement between the data measured in the present work and that reported in the literature. The higher value of $\log K_1$ reported in [17] could be due to the different ionic strengths used in the experiment. There are no literature data on ΔH for U(VI)–maleate and U(VI)–fumarate. The $\log K_{P1}$ and $\log K_{P2}$ for maleic acid are close to those for phthalic acid. It was observed that the $\log K_1$ and $\log K_2$ for U(VI)–maleate complexes are quite close to those for U(VI)–phthalates [10]. This indicates strong correlation between $\log K$ of the complex and $\log K_P$ of the carboxylic acid. The ΔH for U(VI) complexes with aliphatic seven membered di-carboxylates, like succinate, has been reported (15 and 21 kJ/mol) by different groups [10,32]. Analogous to Eu(III)–maleate and Eu(III)–succinate, compensating effect of basicity and rigid ligand structure has also been observed in case of U(VI) complexes. The plot of $\log K_1$ vs. $\log K_P$ suggests, similar to Eu(III)–fumarate, charge polarization in fumarate molecule upon complexation with UO_2^{2+} (Fig. 5b) [33].

Comparison of the $\log K_1$ for Eu(III) and U(VI) complexes with maleate and fumarate (Table 4) shows that the $\log K_1$ values are higher for U(VI) than that for Eu(III). This can be explained in terms of the higher effective charge (3.33) of UO_2^{2+} than that of Eu^{3+}. The higher endothermic enthalpy of formation of U(VI)–maleate than Eu(III)–maleate suggests greater dehydration of uranyl ion during complexation which is also reflected in the higher entropy

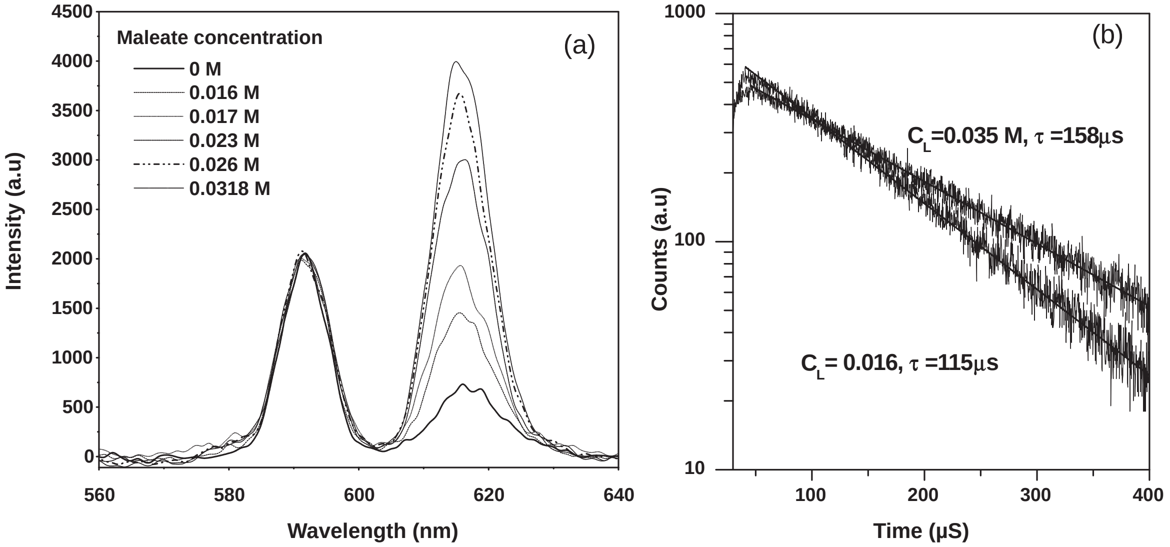

Fig. 6. (a) Normalized fluorescence emission spectra of Eu(III) as a function of increasing maleate concentration and (b) decay of fluorescence emission at two different concentrations of ligand (0.016 M and 0.035 M) (Cup solution: 2.7 ml Eu(III) (5 mM in 0.016 M $HClO_4$), titrant: maleate solution (C_L = 0.500 M and C_{OH} = 0.009 M)).

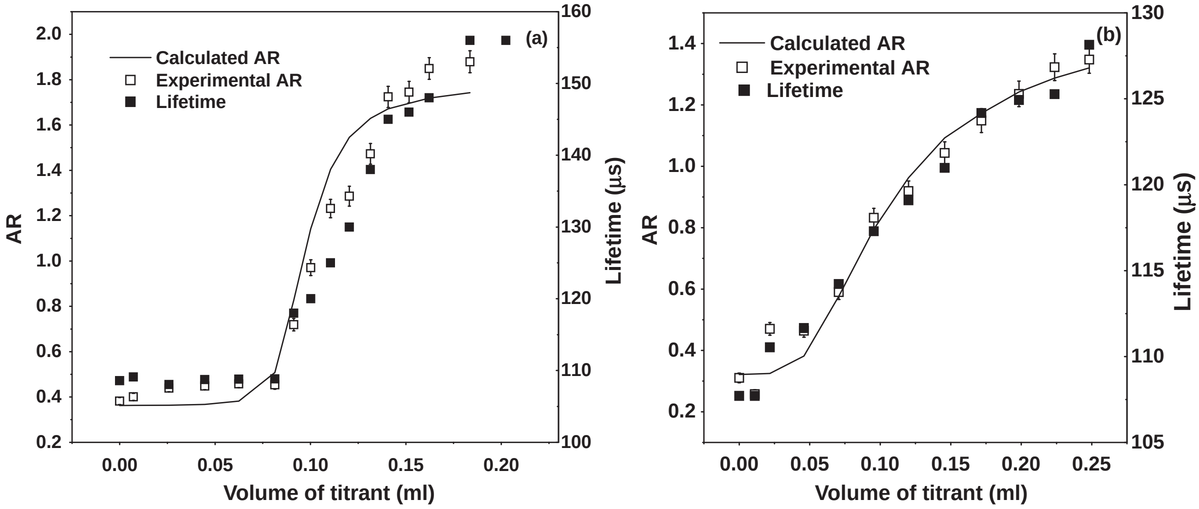

Fig. 7. Variation of AR and fluorescence lifetime with volume of titrant: (a) titration of Eu(III) (5 mM in 0.016 M $HClO_4$) by maleate solution (C_L = 0.500 M and C_{OH} = 0.009 M) and (b) titration of Eu(III) (3 mM in 0.011 M $HClO_4$) by fumarate solution (C_L = 0.500 M and C_H = 0.186 M).

term ($T\Delta S$). In the case of fumarate the endothermic enthalpy is nearly equal for both the metal ions, indicating the expulsion of less number of water molecules to accommodate the monodentate fumarate in the coordination sphere of UO_2^{2+} ion than that in the case of U(VI)–maleate wherein a 7 membered chelate ring is formed in the complex. The higher dehydration energy in U(VI)–fumarate seems to have been compensated by higher interaction of U(VI) and fumarate.

Table 4 show that the maleate complexes for both the metal ions are more stable than fumarate complexes, with the difference in the log K_1 of maleate and fumarate being more in the case of U(VI) than that in the case of Eu(III). The ΔH value for the 1:1 maleate and fumarate complexes is nearly same in the case of Eu(III) while in the case of U(VI) the same is higher for maleate than fumarate. Thus, in the case of Eu(III) the complexation is mainly governed by the entropy factor, while in the case of U(VI) enthalpy factor also plays an important role. This can be explained in terms of the extent of dehydration of metal ion required to accommodate the ligand in the coordination space. In the case of U(VI) the carboxylate ligand is distributed spatially in the equatorial plane of the $[O{=}U{=}O]^{2+}$ ion, thereby necessitating the expulsion of more number of rigidly held water molecules than that in the case of Eu(III), wherein the stearic strain on the ligand is much less. The higher dehydration of UO_2^{2+} by maleate ion results in higher entropy and enthalpy of complexation in U(VI) maleate compared to fumarate. Thus, the effect of chelation and ligand volume is reflected more in thermodynamic parameters of U(VI) than Eu(III). Similar observation were made by Kirishima et al. in case of U(VI) complex with dicarboxylates of different chain lengths [10]. However, this can be confirmed by measurement of the local structure around the metal ions by techniques such as EXAFS.

4. Conclusion

Complexation of Eu(III) and U(VI) by maleate and fumarate is mainly governed by entropy. For the same ligand, U(VI) complex is more stable compared to Eu(III) complex indicating the complexation is governed by electrostatic interactions. The higher endothermicity in the case of U(VI) complexation suggests the greater degree of dehydration required to accommodate the ligand molecule in the equatorial plane of $[O{=}U{=}O]^{2+}$. Thermodynamic parameters suggest charge polarization in fumarate complexes of Eu(III) and U(VI) which has been further supported by theoretical calculations. The higher stability of maleate complexes than fumarate complexes is due to the chelate effect. The fluorescence lifetime data support higher entropy of complexation in the case of Eu(III)–maleate compared to Eu(III)–fumarate.

Acknowledgement

Authors thank Dr. S. V. Godbole for support and cooperation during fluorescence spectroscopy measurements.

References

[1] P.D. Bernardo, P.L. Zanonato, G. Tian, M. Tolazzi, L. Rao, Thermodynamics of the complexation of uranium(VI) with oxalate in aqueous solution at 10–70° C, Dalton Trans. 23 (2009) 4450–4457.
[2] Z. Zhang, G. Helms, S.B. Clark, G. Tian, P.L. Zanonato, L. Rao, Complexation of uranium(VI) by gluconate in acidic solutions: a thermodynamic study with structural analysis, Inorg. Chem. 48 (2009) 3814–3824.
[3] G.J. Vazquez, C.J. Dodge, A.J. Francis, Interaction of uranium(VI) with phthalic acid, Inorg. Chem. 47 (2008) 10739–10743.
[4] L. Rao, P.L. Zanonato, P.D. Bernardo, Interaction of actinides with carboxylates in solution: complexation of U(VI), Th(IV)and Nd(III) with acetate at variable temperatures, J. Nucl. Radiochim. Sci. 6 (2005) 31–37.
[5] N. Rawat, S. Kumar, B.S. Tomar, The time differential perturbed angular correlation study of binding of hafnium to humic acid and its model compound, Polyhedron 28 (2009) 1399–1402.
[6] A. Jain, K. Yadav, M. Mohapatra, S.V. Godbole, B.S. Tomar, Spectroscopic investigation on europium complexation with humic acid and its model compounds, Spectrochim. Acta A 72 (2009) 1122–1126.
[7] F. Pelle, P. Aschehoug, S. Surble, F. Millange, C. Serre, G. Ferey, Interactions between Eu^{3+} ions in inorganic–organic hybrid materials, J. Solid State Chem. 183 (2010) 795–802.
[8] C. Serre, F. Pelle, N. Gardant, G. Ferey, Synthesis and characterization of MIL-79 and MIL-80: two new luminescent open-framework rare-earth dicarboxylates with unusual 1D inorganic subnetworks, Chem. Mater. 16 (2004) 1177–1182.
[9] C.N.R. Rao, S. Natarajan, R. Vaidhyanathan, Metal carboxylates with open architectures, Angew. Chem. Int. Ed. 43 (2004) 1466–1496.
[10] A. Kirishima, Y. Onishi, N. Sato, O. Tochiyama, Thermodynamic study on the U(VI) complexation with dicarboxylates by calorimetry, Radiochim. Acta 96 (2008) 581–589.
[11] H. Kitano, Y. Onishi, A. Kirishima, N. Sato, O. Tochiyama, Determination of the thermodynamic quantities of complexation between Eu(III) and carboxylic acids by microcalorimetry, Radiochim. Acta 94 (2006) 541–547.
[12] N. Rawat, R.S. Sharma, B.S. Tomar, V.K. Manchanda, Thermodynamic study of complexation of Eu(III) with carboxylates by potentiometry and calorimetry, Thermochim. Acta 501 (2010) 13–18.
[13] B. Brendebach, N.L. Banik, Ch.M. Marquardt, J. Rothe, M.A. Denecke, H. Geckeis, X-ray absorption spectroscopic study of trivalent and tetravalent actinides in solution at varying pH values, Radiochim. Acta 97 (2009) 701–708.
[14] P. Thakur, J.N. Mathur, C.J. Dodge, A.J. Francis, G.R. Choppin, Thermodynamics and the structural aspects of the ternary complexes of Am(III), Cm(III) and Eu(III) with OX and EDTA + OX, Dalton Trans. 40 (2006) 4829–4837.
[15] H. Moll, G. Geipel, T. Reich, G. Bernhard, T. Fanghanel, I. Grenthe, Uranyl(VI) complexes with alpha-substituted carboxylic acids in aqueous solution, Radiochim. Acta 91 (2003) 11–20.
[16] G.R. Choppin, A. Dadgar, R. Stampfli, The thermodynamics of lanthanide complexing by fumarate and maleate, J. Inorg. Nucl. Chem. 34 (1972) 875–880.
[17] S. Ramamoorthy, M. Santappa, Stability constants of some uranyl complexes, Bull. Chem. Soc. Japan 42 (1969) 411–416.
[18] P. Gans, B. O'Sullivan, GLEE, a new computer program for glass electrode calibration, Talanta 51 (2000) 33–37.
[19] P. Gans, A. Sabatini, A. Vacca, Investigation of equilibria in solution: determination of equilibrium constant with the HYPERQUAD suite of programs, Talanta 43 (1996) 1739–1753.
[20] N. Rawat, R.B. Gujar, M.S. Murali, B.S. Tomar, V.K. Manchanda, Thermodynamics of complexation of Sr(II) and Ba(II) by 18 crown 6 in water–ethanol binary mixture using titration calorimetry, Thermochim. Acta 488 (2009) 21–26.
[21] R. Ahlrichs, M. Bär, M. Häser, H. Horn, C. Kölmel, TURBOMOLE is program package developed by the Quantum Chemistry Group at the University of Karlsruhe, Germany, Chem. Phys. Lett. 162 (1989) 165–169.
[22] M. Dolg, H. Stoll, H. Preuss, Energy-adjusted ab initio pseudopotentials for the rare earth elements, J. Chem. Phys. 90 (1989) 1730–1734.
[23] X. Cao, M. Dolg, Valence basis sets for relativistic energy-consistent small-core lanthanide pseudopotentials, J. Chem. Phys. 115 (2001) 7348–7355.
[24] W. Kuchle, M. Dolg, H. Stoll, H. Preuss, Energy-adjusted pseudopotentials for the actinides. Parameter sets and test calculations for thorium and thorium monoxide, J. Chem. Phys. 100 (1994) 7535–7542.
[25] X. Cao, M. Dolg, H. Stoll, Valence basis sets for relativistic energy-consistent small-core actinide pseudopotentials, J. Chem. Phys. 118 (2003) 487–496.
[26] X. Cao, M. Dolg, Segmented contraction scheme for small-core actinide pseudopotential basis sets, J. Mol. Struct. (Theochem) 673 (2004) 203–209.
[27] A.D. Becke, Density-functional exchange—energy approximation with correct asymptotic behavior, Phys. Rev. A 38 (1988) 3098–3100.
[28] J.P. Perdew, Density-functional approximation for the correlation energy of the inhomogeneous electron gas, Phys. Rev. B 33 (1986) 8822–8824.
[29] J. Huskens, H. Van Bekkum, J.A. Peters, G.R. Choppin, Coordination of monocarboxylates in lanthanide(III) complexes, Inorg. Chim. Acta 245 (1996) 51–57.
[30] T. Kimura, G.R. Choppin, Luminescence study on determination of the hydration number of Cm(III), J. Alloys Compd. 213/214 (1994) 313–317.
[31] K.S. Rajan, J. Martell, Equilibrium studies of uranyl complexes-IV, reactions with carboxylic acids, Inorg. Nucl. Chem. 29 (1967) 523–529.
[32] A. Bismond, A. Cassol, P. Di Bernard, L. Magon, G. Tomat, Thermodynamic properties of actinide complexes. VII. Uranyl(VI)–succinate system, Inorg. Nucl. Chem. Lett. 17 (1981) 79–81.
[33] L. Rao, A.Y. Garnov, D. Rai, Y. Xia, R.C. Moore, Protonation and complexation of isosaccharinic acid with U(VI) and Fe(III) in acidic solutions: potentiometric and calorimetric studies, Radiochim. Acta 92 (2004) 575–581.